J Neuropathol Exp Neurol
Vol. 68, No. 11
November 2009
pp. 1184–1192

ORIGINAL ARTICLE

Nuclear Contour Irregularity and Abnormal Transporter Protein Distribution in Anterior Horn Cells in Amyotrophic Lateral Sclerosis

Yoshimi Kinoshita, MD, Hidefumi Ito, MD, PhD, Asao Hirano, MD, Kengo Fujita, MD, PhD, Reika Wate, MD, PhD, Masataka Nakamura, MD, Satoshi Kaneko, MD, PhD, Satoshi Nakano, MD, PhD, and Hirofumi Kusaka, MD, PhD

Abstract

The nucleocytoplasmic transport system is essential for maintaining cell viability; transport of proteins and nucleic acids between the nucleus and the cytoplasm occurs through nuclear pore complexes (NPCs). In this study, we examined the immunohistochemical distribution of the major protein components of NPCs, Nup62, Nup88, and Nup153, in spinal cords from controls and patients with sporadic or familial amyotrophic lateral sclerosis (SALS or FALS) and its mouse model. In control subjects, immunolabeling on the nuclear envelopes of anterior horn cells (AHCs) was invariably smooth and continuous, whereas in SALS and FALS patients, the AHCs predominantly showed irregular nuclear contours. Double immunofluorescence staining demonstrated that in SALS patients, importin-β immunoreactivity was absent in the nuclei in a subset of AHCs; in these cells, Nup62 immunolabeling of nuclear membrane was invariably irregular, suggesting that there was dysfunctional nucleocytoplasmic transport in those AHCs. In the mouse model, Nup62-immunolabeled AHCs with irregular nuclear contours were predominant as early as the presymptomatic stage and the contours became progressively discontinuous along with disease development. Together, these observations suggest that dysfunctional nucleocytoplasmic transport may underlie the pathogenesis of ALS.

Key Words: Amyotrophic lateral sclerosis, Nuclear pore complex, Nuclear contour irregularity, Nucleocytoplasmic transport system, Nucleoporin.

INTRODUCTION

Amyotrophic lateral sclerosis (ALS) is a fatal neurodegenerative disorder characterized by a relentless destruction of motor neurons; it manifests clinically as progressive weakness leading to death within a few years. Approximately 10% of ALS cases are familial. In approximately 15% of these patients, the disease is caused by dominantly inherited mutations in the copper- and zinc-dependent superoxide dismutase (*SOD1*) gene (1). Although several hypotheses have been proposed concerning the pathogenesis of sporadic ALS (SALS) and of familial ALS (FALS), the specific mechanisms remain unclear and effective treatment is not currently available.

We recently reported altered immunohistochemical localization of proteins associated with the nucleocytoplasmic transport system (i.e. importin-β and importin-α) in the lumbar spinal cord of ALS model mice (2). The immunoreactivities of these proteins in the surviving anterior horn cells (AHCs) showed a significant progressive decrease in the nucleus and an increase in the cytoplasm as the disease progressed. In view of these results, we hypothesized that dysfunctional nucleocytoplasmic transport might be involved in the pathogenesis of ALS. Moreover, we demonstrated that certain representative cargo proteins transported into the nucleus in an importin-β/α–dependent, importin-β family-dependent only, or importin-β/α–independent manner showed a similar abnormal distribution as importin-β/α. These findings prompted us to hypothesize that dysfunction of the nuclear pore complexes (NPCs) may underlie this abnormal localization.

The NPC in vertebrates is a 60- to 125-MDa structure spanning the plane of the nuclear envelope and is composed of approximately 30 distinct structural proteins known as nucleoporins (3–6). Among them, Nup358 and Nup88, Nup62, and Nup153, which are in the cytoplasmic, central, and nucleoplasmic regions of the NPC, respectively, have been proposed to provide sequential binding sites for the passage of importin-β into the nucleus (Fig. 1) (7, 8). The importin-β transport complex binds to nucleoporins with progressively increasing affinity as the complex moves from Nup358 to the Nup62 complex and then to Nup153. Therefore, it is assumed that these nucleoporins play an important role in the interactions between the cytoplasmic and nuclear transport processes.

The NPCs have been investigated in certain disorders, for example, primary biliary cirrhosis, neoplasms, and viral infections (9). Little is known, however, about NPCs in neurodegenerative disorders. Sheffield et al (10) recently

From the Department of Neurology (YK, HI, KF, RW, MN, SK, SN, HK), Kansai Medical University, Moriguchi, Osaka; and Department of Neurology (HI), Kyoto University Graduate School of Medicine, Shogoin, Sakyo-ku, Kyoto, Japan; and Division of Neuropathology, Department of Pathology (AH), Montefiore Medical Center, Bronx, New York.
Send correspondence and reprint requests to: Hidefumi Ito, MD, PhD, Department of Neurology, Kyoto University Graduate School of Medicine, 54 Kawahara-cho, Shogoin, Sakyo-ku, Kyoto, 606-8507, Japan; E-mail: itohid@kuhp.kyoto-u.ac.jp

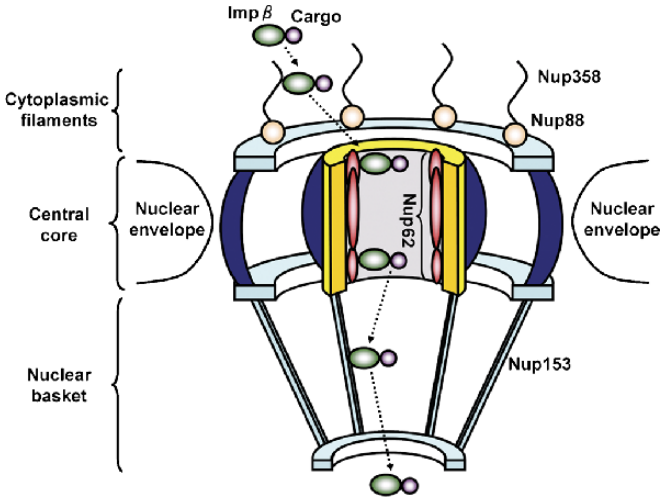

FIGURE 1. Schematic representation of the structure of a nuclear pore complex. The locations of Nup358 and Nup88, components of the cytoplasmic filament, Nup62, a component of the central core, and Nup153, a component of the nuclear basket, are depicted. Impβ, importin-β; Nup, nuclear pore complex proteins.

investigated the potential involvement of nucleoporins and the transport protein nuclear transport factor 2 in Alzheimer disease (AD), but no information is currently available regarding NPCs in ALS.

In this study, we investigated the distribution of nucleoporins and importin-β in the spinal cord of SALS and FALS patients and in ALS model mice.

MATERIALS AND METHODS

Lumbar spinal cord tissue was obtained from clinically and neuropathologically proven SALS (7 cases) and FALS (4 cases) patients; the latter had a confirmed heterozygous 1-amino acid substitution in the gene encoding SOD1 (3 patients with an alanine to valine substitution at codon 4 (A4V) (11) and 1 case with an isoleucine to threonine substitution at codon 113 (I113T). The spinal cords from 6 age-matched neurologically and neuropathologically normal individuals served as controls. The clinical profiles of these cases are summarized in Table 1. The spinal cords were fixed for several weeks in 10% neutral formalin, sliced, embedded in paraffin, and cut into 7-μm-thick sections.

For mouse tissue samples, founder male mice heterozygous for the ALS-linked G93A mutation of the human gene for SOD1 (TgN[B6SJL-Tg{SOD1-G93A}1Gur]) (12) and female nontransgenic B6SJLF1/J mice originally obtained from the Jackson Laboratory (Bar Harbor, ME) were crossed in the Kansai Medical University animal facility. All animal breeding and the experimental protocols were approved by the Institutional Committee for Animal Safety and Welfare of Kansai Medical University and are in agreement with the Guidelines from the National Institutes of Health on the use of live animals. Animals were genotyped using an ASTEC research thermal cycler for polymerase chain reaction amplification of mouse DNA extracted from tail snips as previously described (1, 13).

G93A SOD1 transgenic (Tg) female mice (n = 5) were used in each of 4 age groups as follows: 8 to 11 weeks (presymptomatic stage of the progression of the motor dysfunction); 12 to 14 weeks (early symptomatic); 15 to

TABLE 1. Clinical Data

Case	Age, Years	Sex	Postmortem Delay, Hours	Diagnosis	Duration of ALS, Months
ALS					
1	81	F	6.5	SALS	12
2	63	M	5.5	SALS	14
3	72	F	3.5	SALS	20
4	77	M	6.0	SALS	24
5	64	M	3.0	SALS	27
6	64	F	5.0	SALS	39
7	67	M	505	SALS	72*
8	39	M	Unknown	FALS (Ala4Val)	7
9	46	M	Unknown	FALS (Ala4Val)	8
10	66	M	Unknown	FALS (Ala4Val)	24
11	64	M	5.5	FALS (I113T)	6
Control					
12	63	F	3.0	Gastric cancer	
13	74	F	3.5	Gastric cancer	
14	68	M	6.5	Pancreatic cancer	
15	79	M	4.0	Malignant lymphoma	
16	56	M	7.0	Hepatocellular carcinoma	
17	79	F	3.0	Dissecting aneurysm	

*Patient no. 7 was on artificial ventilation for 48 months.
ALS, amyotrophic lateral sclerosis; F, female; FALS, familial ALS with indicated mutation; M, male; SALS, sporadic ALS.

17 weeks (middle symptomatic); and 18 to 20 weeks (late symptomatic). Female wild-type (Wt) littermates at 8 to 20 weeks of age (n = 20) served as controls. Under deep anesthesia with diethyl ether, each mouse was perfused through a cardiac cannula with 4% paraformaldehyde in 0.1 mol/L PBS as a fixative. The spinal cords were dissected, and their lumbar regions were embedded in paraffin and sectioned transversely at a thickness of 7 μm.

The human and murine sections were deparaffinized and stained with hematoxylin and eosin (H&E). After having been photographed, the sections were decolorized and then immunostained with a mouse monoclonal antibody (mAb) against Nup62 (BD Transduction, San Diego, CA) diluted 1:1000 for mouse sections, 1:500 for human sections), mouse anti-Nup88 mAb (BD Transduction) was used at 1:1000 after pretreatment with 98.0% formic acid (Wako, Osaka, Japan) for 5 minutes at room temperature; mouse anti-Nup153 mAb (1:250; Abcam Inc, Cambridge, MA) was used after pretreatment with heat retrieval for 5 minutes in 10 mmol/L citrate buffer in a microwave oven.

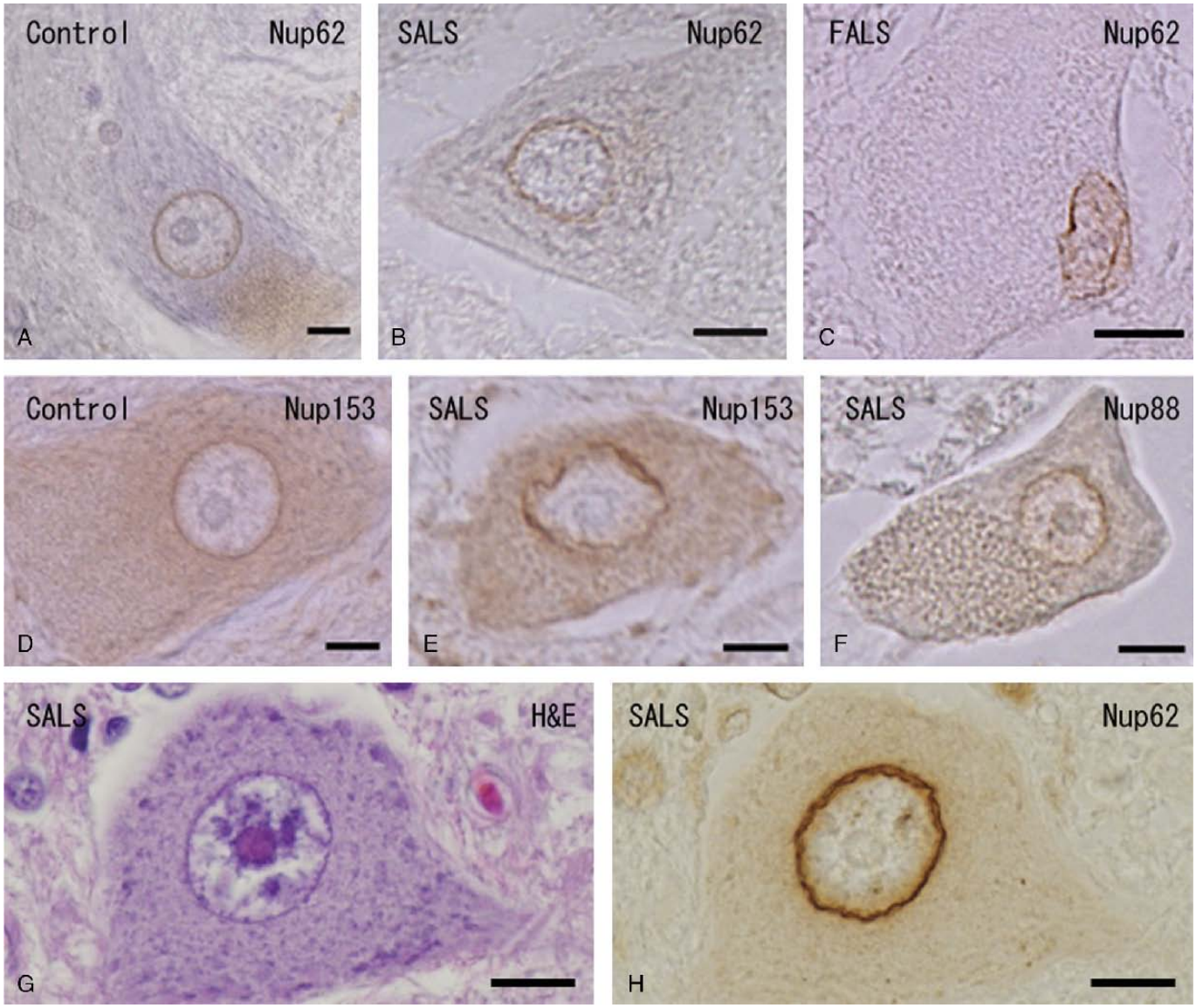

FIGURE 2. Lumbar spinal anterior horn cells (AHCs) from control subjects **(A, D)**, patients with spontaneous amyotrophic lateral sclerosis (SALS) **(B, E–H)**, and from a case of familial ALS with the A4V SOD1 mutation **(C)**. **(A, D)** The AHCs of the controls show entirely smooth nuclear contours when they are immunostained for Nup62 or Nup153. **(B, E, F)** The AHCs of SALS cases show tortuous and redundant nuclear contours when they are immunostained for Nup62, Nup153, and Nup 88. **(C)** An AHC of a familial ALS (FALS) patient shows an irregular nuclear rim with Nup62 immunohistochemistry. **(G, H)** An AHC with a normal-looking nucleus by H&E **(G)** was decolorized and immunostained for Nup62 **(H)**, demonstrating an irregularly redundant nuclear contour. Immunohistochemistry for Nup62 **(A, B, C, H)**, for Nup153 **(D, E)**, and for Nup88 **(F)**. Scale bars = 10 μm.

Incubation was carried out overnight at 4°C. Bound primary antibody was detected with the appropriate Vectastain Elite ABC kit (Vector Laboratories, Burlingame, CA); 3,3′-diaminobenzidine tetrahydrochloride was used as the chromogen. Sections from the Tg mice also stained with anti-active caspase-3 antibody (rabbit polyclonal, 1:40,000, BD PharMingen, San Diego, CA) after pretreatment with heat retrieval were photographed and then restained with the anti-Nup62 antibody.

Double immunofluorescence staining on lumbar sections from control and SALS cases was performed using the anti–importin-β antibody (mouse mAb, 1:50; BD Bioscience) and anti-Nup62 antibody (1:100). These primary antibodies were detected with Alexa Fluor 546 goat anti-rabbit IgG (1:200; Molecular Probes, Eugene, OR) and Alexa Fluor 488 goat anti-mouse IgG (1:200; Molecular Probes). The slides were mounted with Vectashield (Vector) and observed with a Zeiss LSM 510 META confocal microscope.

Staining specificity was assessed by substituting the primary antibodies with the appropriate amount of nonimmune serum or PBS solution containing 3% bovine serum albumin or by preincubating the primary antibodies with an excess of the peptide immunogen. No reaction product was seen in these control sections (not shown).

Under 400× magnification, we investigated nonadjacent sections immunostained with the anti-Nup62 antibody that provided optimal labeling with low background and classified the AHCs with clearly visible nucleoli into those having smooth or irregular nuclear contours. When there was a ruffled edge or redundant or tortuous contour, the nucleus was classified as *irregular*. The nuclear contours of AHCs that had nuclei larger than 15 and 10 μm in diameter in human and murine materials, respectively, were evaluated. We further distinguished these AHCs with irregular nuclear contours into those with nuclear rims with continuous (i.e. entire) and with discontinuous staining.

The mean and SDs of the cell count for each of these 3 categories in 3 sections from each of the patients with SALS or FALS and the control cases and in 5 sections from each of the mouse groups were determined; we then calculated the percentage of cells in each category. Statistical analysis of the mean percentage of each category in the Tg and Wt mice was carried out using Student *t*-test.

RESULTS

The antibodies against Nup62, Nup88, and Nup153 gave similar immunohistochemical results in sections from

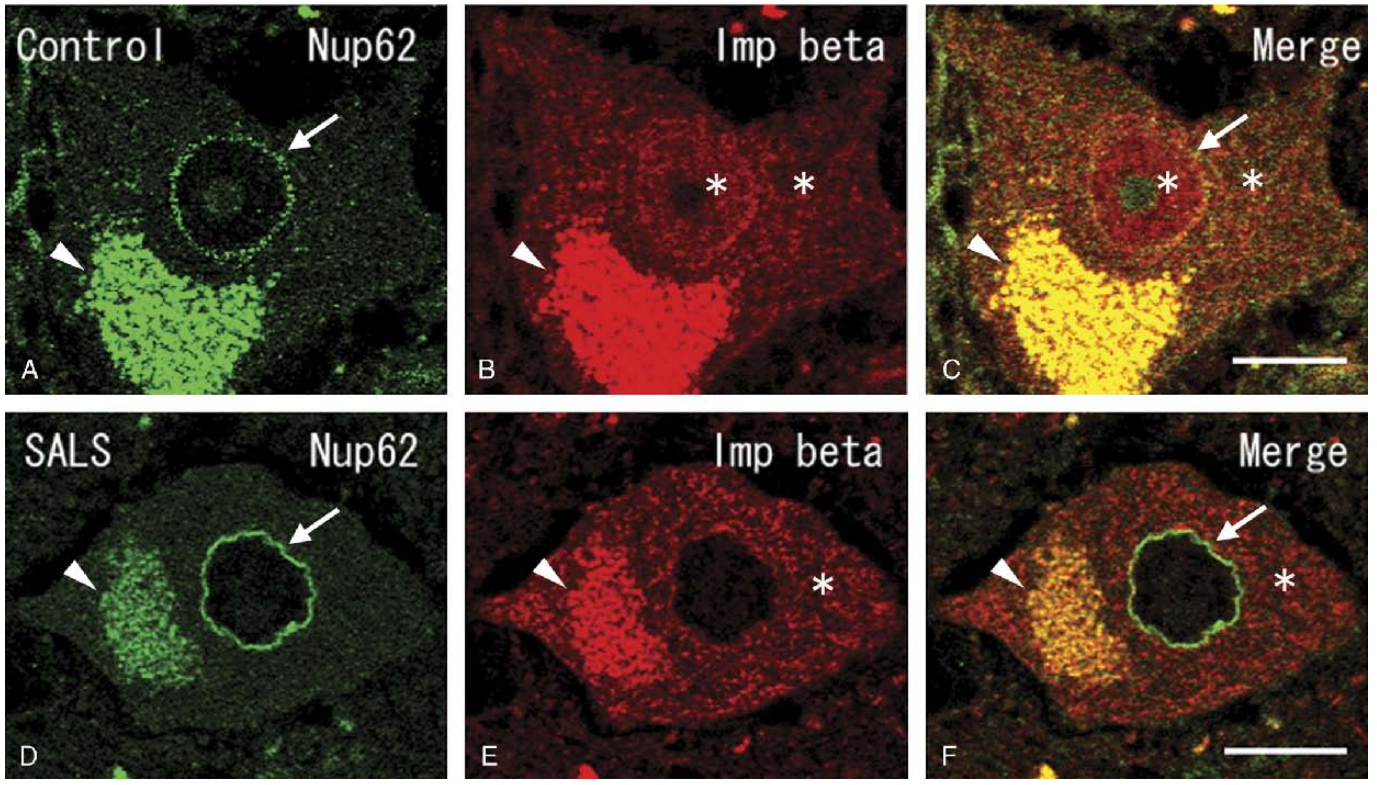

FIGURE 3. Double immunofluorescence staining of lumbar anterior horn cells (AHCs) from a control case **(A–C)** and from a spontaneous ALS (SALS) case **(D–F)** immunostained for Nup62 (green) and importin-β (red). **(A–C)** The AHCs of the control case show a diffuse or granular pattern of importin-β immunoreactivity within both the nucleus and cytoplasm (asterisks in **[B]** and **[C]**); the nuclear rim labeled with anti-Nup62 seems smooth and has a continuous arrangement of punctate immunoreaction product (arrows in **[A]** and **[C]**). **(D–F)** In the AHCs of the SALS case, there is immunoreactivity for importin-β within the cytoplasm (asterisks in **[E]** and **[F]**) but is entirely absent from the nucleus; the nucleus has an irregular tortuous contour with the anti-Nup62 antibody (arrows in **[D]** and **[F]**). Arrowheads in all panels indicate autofluorescence of lipofuscin. Scale bars = 20 μm.

TABLE 2. Frequency of Nucleoporin-Immunolabeled Nuclear Contour Patterns of Anterior Horn Cells

	Patterns		
	Smooth	Irregular	
Cases	Continuous	Continuous	Discontinuous
SALS			
1	5.3 ± 0.6 (53.0%)	4.7 ± 4.7 (47.0%)	0 (0%)
2	0 (0%)	7.3 ± 2.9 (100%)	0 (0%)
3	0 (0%)	7.7 ± 2.1 (100%)	0 (0%)
4	0 (0%)	7.3 ± 2.1 (100%)	0 (0%)
5	1.0 ± 0.0 (10.8%)	8.3 ± 1.5 (89.2%)	0 (0%)
6	1.0 ± 1.4 (12.5%)	7.0 ± 1.4 (87.5%)	0 (0%)
7	0 (0%)	3.0 ± 1.0 (75.0%)	1.0 ± 0.6 (25.0%)
FALS			
8	0 (0%)	2.0 ± 0.0 (100%)	0 (0%)
9	0 (0%)	1.5 ± 0.7 (100%)	0 (0%)
10	0 (0%)	1.0 ± 0.0 (100%)	0 (0%)
Controls			
11	0.8 ± 0.8 (16.0%)	4.2 ± 2.5 (84.0%)	
12	13.0 ± 1.4 (100.0%)	0 (0%)	0 (0%)
13	16.5 ± 3.5 (100.0%)	0 (0%)	0 (0%)
14	13.5 ± 0.7 (100.0%)	0 (0%)	0 (0%)
15	17.0 ± 2.8 (100.0%)	0 (0%)	0 (0%)
16	7.5 ± 0.7 (100.0%)	0 (0%)	0 (0%)
17	12.5 ± 0.7 (100.0%)	0 (0%)	0 (0%)

Data are expressed as mean ± SD. Values in parentheses indicate the percentages of patterns in each case.

FALS, familial amyotrophic lateral sclerosis; SALS, sporadic ALS.

control subjects, SALS and FALS cases, and the Tg and Wt mice. In control individuals, immunoreactivities for these nucleoporins were observed as entirely smooth nuclear contours in all AHCs investigated (Figs. 2A, D), whereas the AHCs of both the SALS and the FALS patients predominantly had redundant or tortuous nuclear contours with ruffled edges; these were defined as having an irregular nuclear contour (Figs. 2B, C, E, F). Notably, the nucleoporin-immunolabeled nuclear irregularity was observed even on normal-looking H&E-stained AHC nuclei after destaining and restaining with anti-Nup62 (Figs. 2G, H).

Double immunofluorescence revealed that the AHC of the controls showed immunoreactivity for importin-β within both the cytoplasm and the nucleus, although the staining intensity of each varied; their nuclear envelopes labeled for Nup62 showed smooth contours (Figs. 3A–C). By contrast, the AHCs in SALS patients that showed irregular nuclear contours with the anti-Nup62 antibody invariably lacked immunoreactivity for importin-β within their nuclei (Figs. 3D–F). The small numbers of the remaining AHCs with smooth nuclear contours in these patients showed immunostaining patterns for importin-β similar to those of the controls. These findings are consistent with our previous observations that in ALS model mice, importin-β immunoreactivity is decreased within the nuclei and increased within the cytoplasm of a subset of the surviving AHCs (2).

Semiquantitative analysis of the lumbar AHCs stained with anti-Nup62 antibody revealed that all of the AHCs observed in the control subjects had smooth nuclear contours (Table 2). By contrast, in 6 patients of the 7 SALS

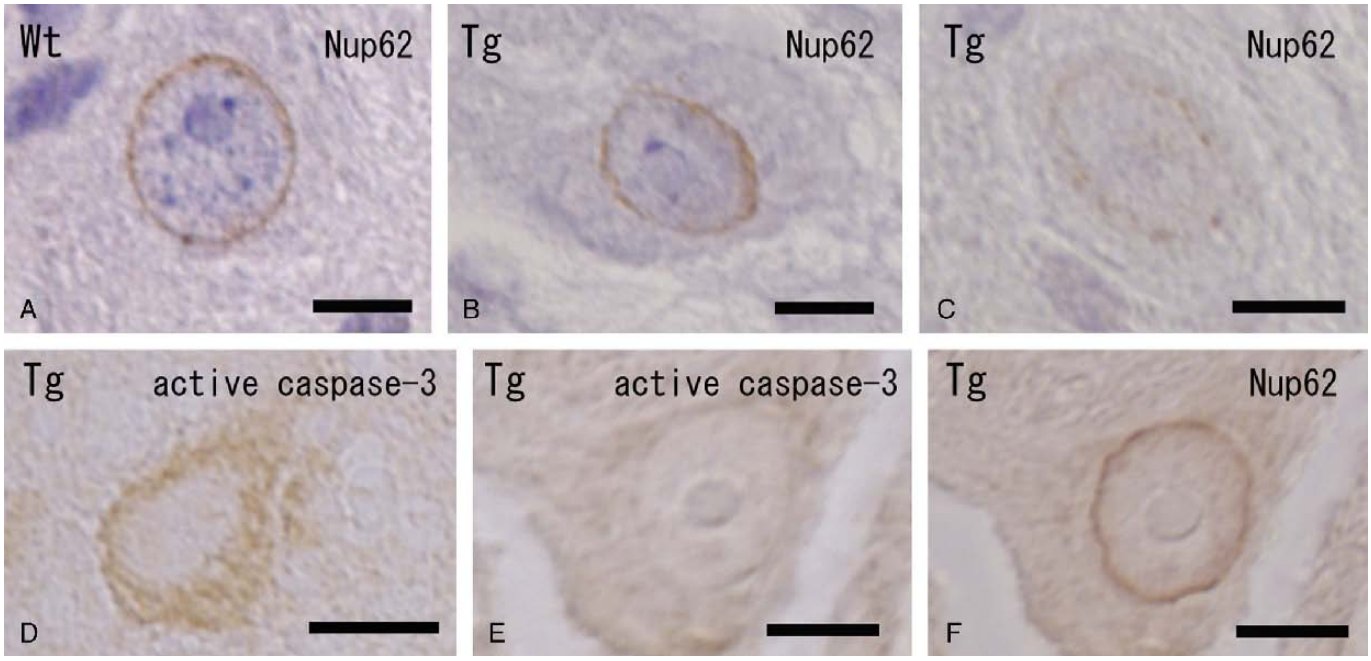

FIGURE 4. Lumbar spinal anterior horn cells (AHCs) of wild-type (Wt) mouse **(A)** and G93A mutant superoxide dismutase-1 transgenic (Tg) mice **(B–F)**. Nup62 immunohistochemistry differentiates AHCs with a smooth contour in the control mouse **(A)**, and irregular and continuous **(B)** and irregular and discontinuous **(C)** nuclear contours in Tg mice. **(D)** Antibody to active caspase-3 immunostains the cytoplasm of an AHC from a 10-week-old Tg mouse. **(E)** An AHC of a Tg mouse of the same age as the Wt mouse shown in **(A)** had no reactivity for active caspase-3. **(F)** The neuron in **(E)** was restained with the anti-Nup62 antibody and has an irregular nuclear contour. Scale bars = 10 μm.

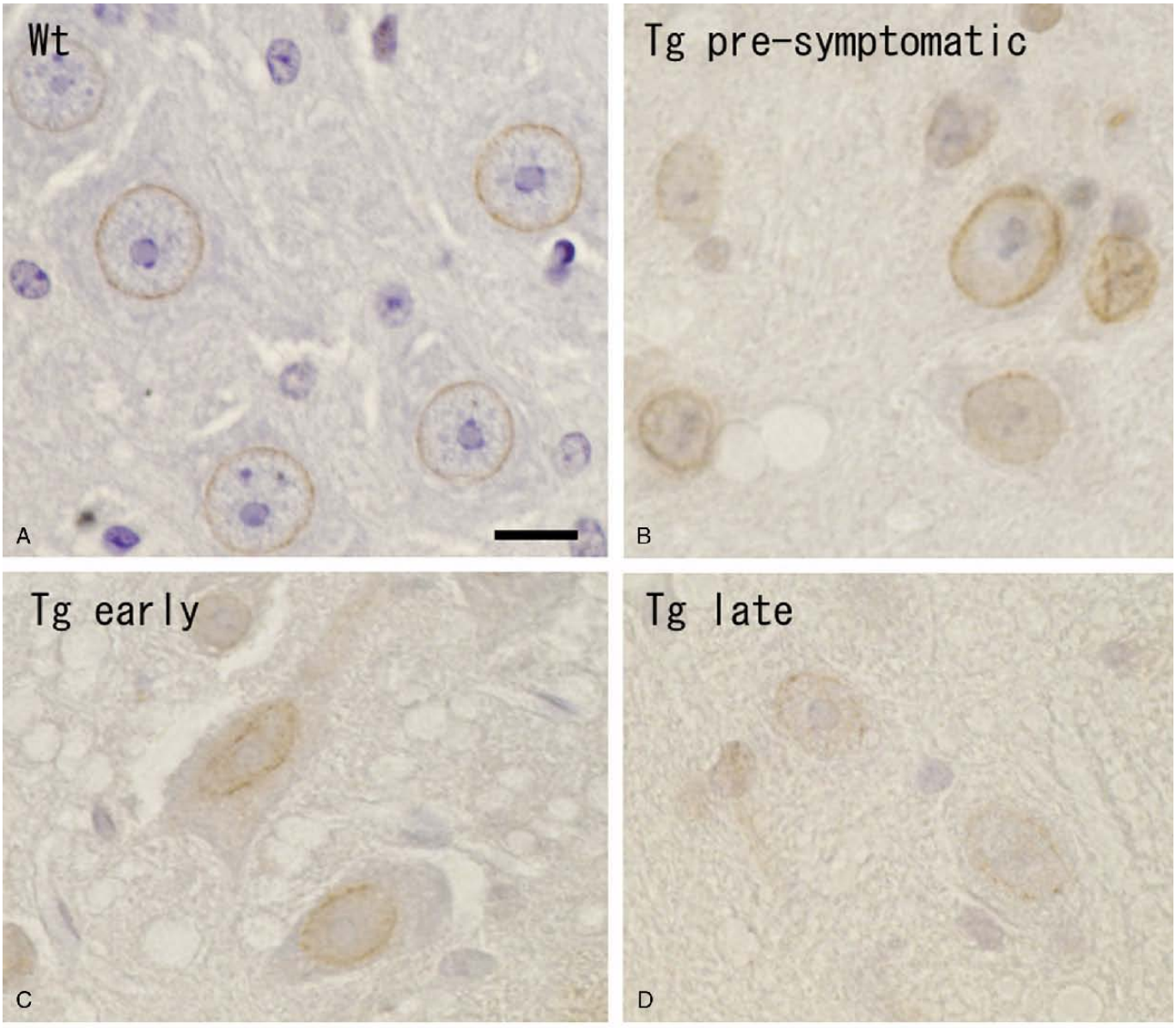

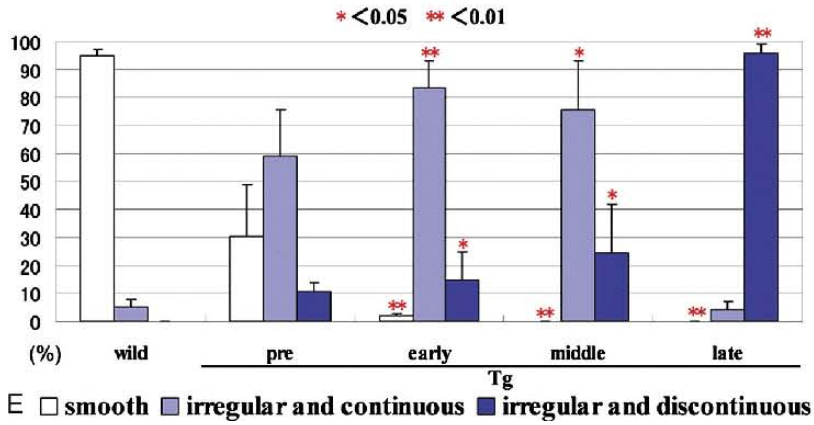

(Cases 2–7), more than 87.5% of the AHCs had irregular nuclear rims. In Case 1, the lumbar AHCs with smooth contours were more frequent (53.0%) than those in the other SALS cases. This patient presented with bulbar palsy at the onset of disease and died because of respiratory failure after a short clinical course (12 months). She was ambulatory until death, suggesting that the lumbar spinal cord might be less affected at autopsy. On the other hand, in Case 7, whose total duration was 72 months (including 48 months under artificial ventilation), several AHCs showed irregular/discontinuous nuclear contours in addition to the irregular/continuous nuclear contours. Irrespective of the type of mutation, most of the AHCs in the FALS cases had irregular/continuous nuclear contours similar to those in most of the SALS cases (Table 2).

In all of the ALS patients, skeinlike or round hyaline inclusions in SALS and Lewy body-like hyaline inclusions (Cases 8–10) or conglomerate inclusions (Case 11) in FALS were recognized in the cytoplasm and the neurites of AHCs. The nuclear contours of the AHC with a visible nucleolus and possessing these inclusions were invariably irregular with anti-Nup62 antibody (100% ± 0%), although the number of such AHCs was sparse per section in all of the patients. On the other hand, the percentages (mean ± SD) of AHCs devoid of visible inclusions but having an irregular nuclear contour in SALS and FALS were 88.3% ± 20.8% and 95.3% ± 9.5%, respectively. The prevalence of nuclear irregularities in AHCs with and without inclusions in SALS and FALS were not significantly different ($p = 0.09$ and $p = 0.20$, respectively).

In the Wt mouse AHCs, the immunoreactivities for the nucleoporins were distributed predominantly as smooth nuclear contours (Fig. 4A). The antibodies used for these sections yielded similar immunohistochemical results irrespective of age, indicating that no age-related changes occurred in the immunohistochemical distributions at least in mice aged between 8 and 20 weeks. On the other hand, in the AHCs of Tg mice, there were irregular/continuous (Fig. 4B) and irregular/discontinuous (Fig. 4C) nuclear contours. To investigate a possible correlation between the nuclear contour irregularity and apoptotic processes, we applied a restaining technique using anti-active caspase-3 and anti-Nup62 antibodies to sections from the Tg mice. Active caspase-3 immunoreactivity was observed in the cytoplasm of a subset of the surviving AHCs (Fig. 4D). On restaining, we encountered instances of AHCs with an irregular nuclear rim stained with anti-Nup62 antibody in the same neurons lacking anti-active caspase-3 immunoreactivity (Figs. 4E, F). This finding suggests that the nucleoporin-immunolabeled nuclear irregularity would unlikely be a consequence of apoptosis.

The results of chronological quantitative analysis of the ALS model mice are shown in Figure 5. In the control mice, Nup62 immunoreactivity was observed along the nuclear rims as smooth contours in most of the AHCs. In contrast, the AHCs with smooth nuclear contours from the Tg mice were significantly few as early as in the presymptomatic stage compared with those of the control mice and were not observed at all in the middle and the late symptomatic Tg mice. The percentages of AHCs with smooth nuclear contours were significantly lower in the symptomatic Tg mice, whereas the proportions of AHCs with an irregular and continuous nuclear contour were higher at the presymptomatic stage of Tg mice than that of the Wt mice; they increased to reach a strongly significant difference at the early symptomatic stage and then decreased. The AHCs with an irregular and discontinuous nuclear contour were first recognizable at the presymptomatic stage (the percentage of this type increased to be significantly high at symptom onset) and became the most common type of AHC at the late symptomatic stage. These results imply that the Nup62-immunolabeled nuclear contours become disrupted along with disease progression and parallel our observations in SALS patients.

DISCUSSION

This is the first demonstration of nuclear contour irregularities in the surviving AHCs of SALS and FALS patients and in AHCs of ALS model mice. These abnormalities are associated with an apparent impairment in importation of importin-β into the AHC nuclei. Our results imply that these dysfunctional NPCs could be involved in the pathogenesis underlying ALS.

The nucleoporin-immunolabeled nuclear irregularity identified in our study is very similar to that observed by Sheffield et al (10) in the hippocampal neurons from AD cases. Moreover, these investigators demonstrated abnormal accumulation of nuclear transport factor 2, a protein carrying RanGDP from the cytoplasm into the nucleus, in the cytoplasm of hippocampal pyramidal cells and postulated that faulty NPCs and nucleocytoplasmic transport are involved in the pathogenesis of AD. Nuclear transport factor 2 is known to be actively transported into the nucleus through the NPCs by binding to Nup62 (14), as in the case of importin-β. Taken together, these studies suggest that the

FIGURE 5. Low-power magnifications of anti-Nup62–immunostained lumbar spinal anterior horn cells (AHCs) from wild-type (Wt) **(A)**, presymptomatic transgenic (Tg) **(B)**, early symptomatic Tg **(C)**, and late symptomatic Tg **(D)** mice. **(A)** Nuclear envelopes of all AHCs in the control section have smooth contours. **(B–D)** In the Tg mice, the nuclear contours of AHCs seem irregular and are discontinuous as the disease progresses. **(E)** Semiquantitative analysis of Nup62-immunostained sections. The proportion of AHCs with irregular nuclear contours is higher in the Tg mice even at the presymptomatic stage; AHCs with smooth nuclear contours are less numerous than in the Wt mice. Note that the percentage of AHCs with irregular nuclear contours is significantly greater in the symptomatic Tg mice and that of AHCs with the irregular/discontinuous nuclear rims progressively increased with the disease progression. Scale bars = 10 μm.

nuclear irregularities represent a functional disturbance of NPCs, and that there may be common pathogenetic processes of neurodegeneration in AD and ALS.

We also demonstrated that progressive disruption of the nuclear contours delineated by Nup62 immunohistochemistry correlated with disease progression in ALS model mice. The mechanism responsible for the discontinuous nucleoporin immunolabeling on the nuclear envelope remains to be elucidated, but it might represent a loss of antigenicity because of nucleoporin degeneration or a severely uneven distribution of NPCs on the nuclear membrane. Nevertheless, our findings that the AHCs with irregular nuclear contours in the ALS model mice were increased over controls even at the presymptomatic stages as well as progressing over time suggest that the nucleoporin-immunolabeled nuclear irregularity is related to the pathogenesis.

The NPCs are known to undergo strong modifications, such as disassembly during apoptosis (15, 16), but no clear relationship was identified between the changes in nucleoporin distribution and apoptosis in AD (10). In the present study, we identified instances with nuclear contour irregularity in the absence of immunoreactivity for caspase-3. Activated caspase-3 is one of the effector caspases commonly situated most downstream of several distinct apoptotic cascades. Therefore, AHCs immunopositive for active caspase-3 are assumed to be at the final stage of the caspase cascade in cells undergoing apoptosis. Indeed, nuclear modification might develop at earlier stages of apoptotic cascades. If the nuclear irregularity is a consequence of apoptosis, however, it would be unlikely that the irregular nuclear rim reverses to the smooth contour during the apoptotic process progressing to the stage of caspase-3 activation. We thus consider that, as in AD, the AHC nuclear contour irregularities in ALS may not be related to apoptosis.

Among several hypotheses proposed on the pathogenesis of ALS, we recently postulated that dysfunctional nucleocytoplasmic transport might impair successful transport of beneficial regeneration signals into the nucleus (2). A dysfunctional nucleocytoplasmic transport system has been proposed to operate in triple A syndrome. This rare disorder is caused by mutations in a gene that encodes the nucleoporin ALADIN (17). ALADIN-defective NPCs have an impaired importin-β/α–mediated import pathway and show weak nuclear import of aprataxin, a repair protein for DNA single-stand breaks, and DNA ligase I, which results in increased susceptibility of cells to oxidative stress and leads to the accumulation of damaged DNA and cell death (17). Similarly in ALS and AD, therefore, beneficial regeneration signals may not be transported into the nucleus, thereby resulting in facilitation of neurodegeneration.

We recently demonstrated that the nuclear staining intensity of phosphorylated Smad2/3 was reduced in AHCs with round hyaline inclusions in brain specimens from SALS patients (18). Phosphorylated Smad2/3 is supposed to enter the nucleus by direct interaction with Nup214 and Nup153, components of the NPCs. Therefore, in view of our present findings, the nuclear contour irregularity as a consequence of possible dysfunctional NPCs in ALS might be involved in impairment of phosphorylated Smad2/3 translocation from the cytoplasm to the nucleus. Beneficial transforming growth factor-β signal transduction would therefore be impaired at the step of Smad2/3 translocation into the nucleus in SALS patients.

Recently, transactivation response DNA-binding protein 43 (TDP-43) has been proposed to be involved in the pathogenesis of ALS. Winton et al (19) demonstrated cytoplasmic aggregate formation in cultured cells expressing mutant TDP-43 with defective nuclear localizing signals and speculated that deleterious perturbation of nuclear trafficking and solubility of TDP-43 may be linked to ALS pathogenesis.

More recently, NPCs were reported to deteriorate in an age-related manner, leading to an increase in nuclear permeability and leakage of proteins (20). In that study, the authors demonstrated that a subset of nucleoporins is oxidatively damaged in old cells, suggesting that the accumulation of damage at the NPC might be related to neurodegeneration (20, 21). Further investigations are needed to elucidate the significance of the nuclear contour irregularities and the signal transduction systems involved in the pathogenesis of ALS.

REFERENCES

1. Rosen DR, Siddique T, Patterson D, et al. Mutations in Cu/Zn superoxide dismutase gene are associated with familial amyotrophic lateral sclerosis. Nature 1993;362:59–62
2. Zhang J, Ito H, Wate R, et al. Altered distributions of nucleocytoplasmic transport-related proteins in the spinal cord of a mouse model of amyotrophic lateral sclerosis. Acta Neuropathol 2006;112:673–80
3. Talcott B, Moore MS. Getting across the nuclear pore complex. Trends Cell Biol 1999;9:312–18
4. Cronshaw JM, Krutchinsky AN, Zhang W, et al. Proteomic analysis of the mammalian nuclear pore complex. J Cell Biol 2002;158:915–27
5. Fahrenkrog B, Aebi U. The nuclear pore complex: Nucleocytoplasmic transport and beyond. Nat Rev Mol Cell Biol 2003;4:757–66
6. Fried H, Kutay U. Nucleocytoplasmic transport: Taking an inventory. Cell Mol Life Sci 2003;60:1659–88
7. Ben-Efraim I, Gerace L. Gradient of increasing affinity of importin beta for nucleoporins along the pathway of nuclear import. J Cell Biol 2001;152:411–17
8. Schwarz-Herion K, Maco B, Sauder U, et al. Domain topology of the p62 complex within the 3-D architecture of the nuclear pore complex. J Mol Biol 2007;370:796–806
9. Cronshaw JM, Matunis MJ. The nuclear pore complex: Disease associations and functional correlations. Trends Endocrinol Metab 2004;15:34–39
10. Sheffield LG, Miskiewicz HB, Tannenbaum LB, et al. Nuclear pore complex proteins in Alzheimer disease. J Neuropathol Exp Neurol 2006;65:45–54
11. Hirano A, Kurland LT, Sayre GP. Familial amyotrophic lateral sclerosis. A subgroup characterized by posterior and spinocerebellar tract involvement and hyaline inclusions in the anterior horn cells. Arch Neurol 1967;16:232–43
12. Gurney ME, Pu H, Chiu AY, et al. Motor neuron degeneration in mice that express a human Cu, Zn superoxide dismutase mutation. Science 1994;264:1772–75
13. Wate R, Ito H, Zhang JH, et al. Expression of an endoplasmic reticulum–resident chaperone, glucose-regulated stress protein 78, in the spinal cord of a mouse model of amyotrophic lateral sclerosis. Acta Neuropathol 2005;110:557–62
14. Paschal BM, Gerace L. Identification of NTF2, a cytosolic factor for nuclear import that interacts with nuclear pore complex protein p62. J Cell Biol 1995;129:925–37

15. Buendia B, Santa-Maria A, Courvalin JC. Caspase-dependent proteolysis of integral and peripheral proteins of nuclear membranes and nuclear pore complex proteins during apoptosis. J Cell Sci 1999;112: 1743–53
16. Kihlmark M, Imreh G, Hallberg E. Sequential degradation of proteins from the nuclear envelope during apoptosis. J Cell Sci 2001;114: 3643–53
17. Hirano M, Furiya Y, Asai H, et al. ALADINI482S causes selective failure of nuclear protein import and hypersensitivity to oxidative stress in triple A syndrome. Proc Natl Acad Sci USA 2006;103:2298–303
18. Nakamura M, Ito H, Wate R, et al. Phosphorylated Smad2/3 immunoreactivity in sporadic and familial amyotrophic lateral sclerosis and its mouse model. Acta Neuropathol 2008;115:327–34
19. Winton MJ, Igaz LM, Wong MM, et al. Disturbance of nuclear and cytoplasmic TAR DNA-binding protein (TDP-43) induces disease-like redistribution, sequestration, and aggregate formation. J Biol Chem 2008;283:13302–9
20. D'Angelo MA, Raices M, Panowski SH, et al. Age-dependent deterioration of nuclear pore complexes causes a loss of nuclear integrity in postmitotic cells. Cell 2009;136:284–95
21. Kotwaliwale CV, Dernburg AF. Old nuclei spring new leaks. Cell 2009; 136:211–12